Vector Chiral Phases in the Frustrated 2D *XY* Model and Quantum Spin Chains

H. Schenck,[1] V. L. Pokrovsky,[2,3] and T. Nattermann[1]

[1]*Institut für Theoretische Physik, Universität zu Köln, Zülpicher Strasse 77, D-50937 Köln, Germany*
[2]*Department of Physics, Texas A&M University, College Station, Texas 77843-4242, USA*
[3]*Landau Institute for Theoretical Physics, Chernogolovka, Moscow District 142432, Russia*

The phase diagram of the frustrated 2D classical and 1D quantum *XY* models is calculated analytically. Four transitions are found: the vortex unbinding transitions triggered by strong fluctuations occur above and below the chiral transition temperature. Vortex interaction is short range on small and logarithmic on large scales. The chiral transition, though belonging to the Ising universality class by symmetry, has different critical exponents due to nonlocal interaction. In a narrow region close to the Lifshitz point a reentrant phase transition between paramagnetic and quasiferromagnetic phase appears. Applications to antiferromagnetic quantum spin chains and multiferroics are discussed.

Introduction.—Landau theory describes phase transitions accompanied by a loss of symmetry. Strong fluctuations lead either to non-mean-field critical behavior or first order transition [1]. The situation is by far less clear in frustrated systems, where discrete and continuous symmetries can be broken simultaneously. Villain, in a seminal work [2], showed that in helical magnets, in addition to the magnetic order, there exists a second, chiral order parameter related to the mutual spin orientation on neighboring sites

$$\boldsymbol{\kappa} = \langle \mathbf{S}_i \times \mathbf{S}_{i+\hat{x}} \rangle. \qquad (1)$$

It soon became clear that many other—interaction or lattice frustrated—models exhibit this type of order as well (see [3–5] for reviews).

The considerations in the present article are restricted to helical magnets for three reasons: (i) they are interesting because of their possible applications as multiferroics [6,7], (ii) they are sufficiently simple to allow controlled analytical approaches, but (iii) still give a rich phase diagram (see Fig. 1).

Villain [8] considered a system of *XY* spins with competing nearest- and next-nearest-neighbor interaction along the $\hat{x}$ axis, which gives rise to helical order with $\boldsymbol{\kappa} = \pm\kappa\hat{x}$. Below we use this helical *XY* (HXY) model as a prototype model of frustrated spin systems. It describes likewise frustrated quantum spin chains at zero temperature, which can be mapped to $1 + 1$-dimensional classical spin models, provided the spin S is large enough [9].

Using mean-field analysis, Villain [8] found a chirally ordered phase above the transition where magnetic order disappears. Whereas in three dimensions more sophisticated renormalization group (RG) methods indicate the existence of a single transition [10], the situation is significantly more complicated in two dimensions.

Here the condensation of topological defects as vortices and domain walls are expected to be relevant mechanisms. Garel and Doniach [11] mapped the HXY model to two coupled *XY* models, resulting in a phase diagram with the chiral transition below the magnetic transition, in contrast to [8]. However, their mapping procedure is doubtful (see [12]). Okwamoto [13] used a self-consistent harmonic approximation (SCHA), which yields a phase diagram of the same topology as in [11], but the dependence of the transition lines on the pitch of the helix is different. Kolezhuk used simple estimates for the energy of the topological defects in a $1 + 1$-dimensional quantum spin chain to find an Onsager-like chiral transition above the *XY* transition, tacitly assuming that the Ising order parameter has a standard local Hamiltonian [12]. Most of the analytical work on quantum spin chains is restricted to the $S = 1/2$ case, where the mapping to our classical model is questionable, or to parameter regions far from those considered in this Letter [14,15].
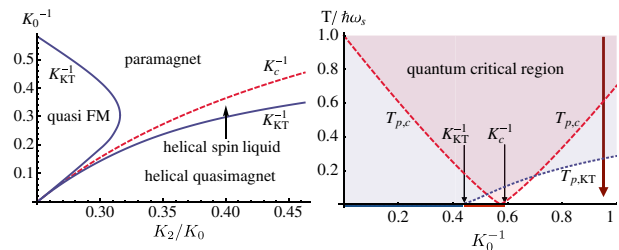

FIG. 1 (color online). Left panel: Phase diagram of the HXY model as a function of K_2/K_0, calculated from (18). The bold lines mark the BKT transition, the dashed line marks the chiral transition. Right panel: Quantum critical regions, $T > T_{p,c}$ for the chiral and $T > T_{p,\mathrm{KT}}$ for the magnetic transition, respectively, of a frustrated quantum spin chain. The thick arrow denotes the parameter region accessible in Gd$(hfac)_3$NITiPr.

Different numerical approaches have been used as well. Hikihara *et al.* [16] considered a spin-1 chain using density matrix RG and obtained, depending on frustration, gapped and gapless chiral phases. These correspond in the 2D classical case to magnetically disordered and quasi-long-range ordered phases, respectively. In extended Monte Carlo studies on the 2D classical HXY model, Cinti *et al.* [17] and Sorokin and Syromyatnikov [18] found transition lines and critical exponents. However, they used an inappropriate finite size scaling analysis [19] which does not take into account the strong anisotropy of systems near the Lifshitz point. As it was shown in [20,21] such anisotropy requires a strong modification of the scaling analysis. Nevertheless, it is possible to extract from their raw data exponents which turn out to be close to ours (see below).

The new features we have found in this model, which distinguish our work from all preceding literature are the following. (i) The nonlocality of the chiral order fluctuations leading to strong modifications of its critical behavior in comparison to 2D Ising model possessing the same symmetry. (ii) The strong anisotropy of the model leading to different scaling behavior in different direction, as known from Lifshitz points. (iii) The anomalous large core of the vortices leads to strong modification of the vortex fugacity.

Our investigation reveals a remarkable simple picture. In the helical ground state both U(1) and parity symmetry are broken. With the degeneracy space SO(2) × $\mathbb{Z}_2$, relevant excitations are spin waves, vortices, and domain walls. Generically, domain walls consist of a regular array of magnetic vortices [22]. At low temperatures spin waves reduce the magnetic order to quasi-long-range (algebraic) order. Spin wave interaction on scales small compared to the chiral correlation length ξ results in nonclassical critical exponents at the chiral transition. Vortices on these scales do not interact. On scales larger than ξ the role of spin waves and vortices interchanges: spin wave interaction becomes irrelevant, whereas the vortex interaction is logarithmic. Reduction of the chiral order at increasing temperatures lowers the energy of vortices, resulting in the Berezinskii-Kosterlitz-Thouless (BKT) transition [1] before the chiral transition takes place. Both phases exhibit a nonzero vector chirality (1). Close to the Lifshitz point there appears a reentrant transition to a quasiferromagnetic phase (see Fig. 1).

The model.—In this Letter we will consider the classical anisotropic *XY* model on a square lattice [23]

$$\bar{\mathcal{H}} = -\sum_i (K_0 \mathbf{S}_i \mathbf{S}_{i+\hat{x}} + K_1 \mathbf{S}_i \mathbf{S}_{i+\hat{y}} - K_2 \mathbf{S}_i \mathbf{S}_{i+2\hat{x}}). \quad (2)$$

Here, $K_n = J_n/T$, K_1, $K_2 > 0$, $\hat{x}$, $\hat{y}$ denotes the unit vector in the x, y direction and the lattice spacing is set equal to unity. In terms of the parameter $k = K_0/4K_2$, the ground

state of (2) is either ferromagnetic ($1 < k$), helical magnetic ($-1 < k < 1$), or antiferromagnetic ($k < -1$). At $k = 0$ the system decays into two independent sublattices which undergo separate BKT transition. Since the Hamiltonian is invariant under the change $K_0 \to -K_0$ and simultaneously flipping all spins on one sublattice of the bipartite lattice, the results for $K_0 < 0$ can be obtained from that for $K_0 > 0$, to which we restrict ourselves now. With $\mathbf{S}_i = (\cos\phi_i, \sin\phi_i)$ the Hamiltonian can be expressed in terms of $\phi_{i+\hat{x}} - \phi_i \to \partial_x\phi \equiv \phi_x$, etc. Assuming for simplicity $K_1 = |K_0|$ we get

$$\bar{\mathcal{H}} = K_0 \int_{\mathbf{x}} \left[\frac{1}{4k}\cos(2\phi_x) - \cos\phi_x + \frac{1}{8k}\phi_{xx}^2 + \frac{1}{2}\phi_y^2 \right], \quad (3)$$

where $\int_{\mathbf{x}} = \int dx dy$. With the ansatz $\phi_x = \theta$ the energy is minimized by $\theta = \pm\arccos k$. Below θ will be considered as a small parameter ensuring the validity of continuous approximation. Then Eq. (3) simplifies to

$$\bar{\mathcal{H}} = \frac{K_0}{2} \int_{\mathbf{x}} \left[-\frac{1}{2}\theta^2\phi_x^2 + \phi_y^2 + \frac{1}{4}(\phi_{xx}^2 + \phi_x^4) \right]. \quad (4)$$

Perturbation theory.—At low temperatures $K_0\theta^2 \gtrsim 1$, the Hamiltonian (4) can be expanded around one of the minima. With $\phi = \pm\theta x + \varphi$ we get

$$\bar{\mathcal{H}} = \frac{K_0}{2} \int_{\mathbf{x}} \left[\theta^2\varphi_x^2 + \varphi_y^2 \pm \theta\varphi_x^3 + \frac{1}{4}(\varphi_{xx}^2 + \varphi_x^4) \right]. \quad (5)$$

For a simple estimate of the anharmonic terms we ignore the compact nature of φ and use $\varphi_x^3 \approx 3\varphi_x\sigma^2$ and $\varphi_x^4 \approx 6\varphi_x^2\sigma^2$ where $\sigma^2 = \langle\varphi_x^2\rangle$. Hence

$$\bar{\mathcal{H}} \approx \frac{K_0}{2} \int_{\mathbf{x}} \left[\left(\theta^2 + \frac{3}{2}\sigma^2\right)(\varphi_x - \delta\theta)^2 + \varphi_y^2 + \frac{1}{4}\varphi_{xx}^2 \right]. \quad (6)$$

$\delta\theta = \mp3\theta\sigma^2/(2\theta^2 + 3\sigma^2)$ represents a temperature dependent correction to the wave vector $\pm\theta\hat{x}$, reducing the modulation. The critical coupling constant $K_0 = K_c$, at which the chiral symmetry is restored, can be estimated from $\delta\theta = \mp O(\theta)$. Alternatively, one can start with the chirally symmetric phase. To lowest order in the anharmonicity, $-\theta^2$ in (4) is replaced by $2r_0 = -\theta^2 + 3\sigma^2(r_0)$,

$$\sigma^2(r) = \frac{1}{4\pi^2 K_0} \int dk_x dk_y k_x^2 \left[rk_x^2 + k_y^2 + \frac{1}{4}k_x^4 \right]^{-1}. \quad (7)$$

With $\sigma(0) = \mathcal{C}_1 K_0^{-1}$, $\mathcal{C}_1 = 0.73$ one gets

$$r_0 \approx \theta^2 t, \qquad t = \frac{K_c}{K_0} - 1, \qquad K_c(\theta) \approx 3\mathcal{C}_1/\theta^2. \quad (8)$$

A variational calculation gives equivalent results.

Vortices.—So far we have neglected the compact nature of the ϕ field. For the further discussion we replace (4) by the effective Hamiltonian

$$\bar{\mathcal{H}} = \frac{K_0}{2} \int_{\mathbf{x}} \left(r\phi_x^2 + \phi_y^2 + \frac{1}{4}\phi_{xx}^2 + \frac{u}{4}N[\phi_x^4] \right). \qquad (9)$$

$N[\phi_x^4] = \phi_x^4 - 6\sigma^2\phi_x^2 + \sigma^4$ denotes the normal product. Apparently, $\xi_x = r^{-1/2}$ and $\xi_y = r^{-1}$ play the role of the correlation length parallel to the x and y direction, respectively. To discuss the nature of vortices, we consider a region of area $L_x L_y$ containing a single vortex. Rescaling the coordinates according to $x/L_x \to x$, $y/L_y \to y$, the linearized saddle point equation reads

$$\lambda_x^2 \phi_{xx} - \frac{1}{4}\lambda_x^4 \phi_{xxxx} + \lambda_y^2 \phi_{yy} = 0, \qquad \lambda_\alpha = \xi_\alpha/L_\alpha. \quad (10)$$

Here we ignored a term $\sim u(\phi_x^2 - \sigma^2)\phi_{xx}$ since the effective (unrescaled) coupling $u_{\text{eff}} \sim L^{-1/2}$ vanishes on large scales (see below).

ϕ can then be decomposed into a spin wave and a vortex contribution, $\phi = \phi^{(sw)} + \phi^{(v)}$, which do not interact. $\phi^{(sw)}$ carries the chiral order and will be treated in the RG calculation below. Since in a vortex configuration $\phi^{(v)}$ is of the order unity, all derivatives in (10) are also of order unity. The vortex solution of Eq. (10) is different in two limiting range of length scales: (i) On small scales, $\lambda_\alpha \gg 1$, one can ignore the first term on the left-hand-side of (10). A variational calculation of the vortex configuration with the ansatz

$$\phi(x, y) = f(\zeta)\theta(x) + [\pi - f(\zeta)]\theta(-x), \qquad (11)$$

where $f(\zeta) = \arcsin\zeta$ and $\zeta = y/\sqrt{\varkappa^2 x^4 + y^2}$, gives $\varkappa = 0.42$ and the vortex energy $\bar{E}_{\text{core}} = 2.38K_0$. From the fact that the energy of these vortices is dominated by *small* scales we conclude that the interaction between the vortices is *short* range, in contrast to the BKT scenario. In this case screening of vortices by vortex pairs on smaller scales is absent. The vortex density is of the order $e^{-\bar{E}_{\text{core}}}$ and hence of the order $e^{-5.24/\theta^2} \ll 1$ below the chiral transition. (ii) In the opposite case of large scales, $\lambda_\alpha \ll 1$, the second term on the left-hand side of (10) is negligible. With the choice $\lambda_x = \lambda_y$ we get standard BKT vortices as solutions.

RG calculation.—The separation of length scales used in the previous paragraph is also relevant to the RG analysis. On small scales $\xi_\alpha \gg L_\alpha$, spin waves strongly interact, implying nonclassical critical exponents at the chiral transition. On the contrary, on large scales $\xi_\alpha \ll L_\alpha$, spin wave interaction becomes irrelevant, whereas vortex interaction leads to the BKT scenario.

We begin with the scales $\xi_\alpha \gg L_\alpha$. $\phi_x \equiv \psi$ plays the role of the order parameter. Equation (9) has the form of a soft spin ψ^4 Ising model, apart from the second term in (9) which can be written as a nonlocal gradient term

$$-\frac{1}{2}\int dx dx' dy |x - x'| \psi_y(x, y)\psi_y(x', y). \qquad (12)$$

Therefore, the critical exponents are expected to be in a universality class different from the Onsager exponents.

We use the standard derivation of the RG flow equations [1] for r, u, K, and the dimensionless vortex fugacity z. Their initial values, defined on the scale of the lattice constant, are $r_0 \ll 1$, $u_0 = 1$, K_0 and $z_0 = \exp(-\bar{E}_{\text{core}})$. To make the model amendable to an $\epsilon = (5/2) - d$ expansion we replace y by a $(d-1)$-dimensional vector $\mathbf{y}$. We first integrate out fluctuations $\phi_{\mathbf{k}}$ of wave vectors limited by inequalities $\pi^2 > (k_x^4/4) + k_y^2 > \pi^2 e^{-2\ell}$ and then rescale according to $x = x' e^{\ell/2}$, $y = y' e^\ell$, $r' = re^\ell$. ϕ as a compact variable as well as u are not rescaled. This leads to the flow equations

$$\frac{d\ln u}{d\ell} = -\frac{\mathcal{C}_2 u}{K}, \qquad \frac{d\ln r}{d\ell} = 1 - \frac{\mathcal{C}_2 u}{3K}. \qquad (13)$$

Here $\mathcal{C}_2 = 9/(2\pi^3)$. Since there is no vortex interaction on these scales, K and z changes only due to rescaling, i.e., $d\ln K/d\ell = -\epsilon$, $d\ln z/d\ell = 3/2$. The rescaling of $z = \exp(-\bar{E}_{\text{core}} + S)$ follows from the vortex entropy $S = \ln[xy/(x'y')] = 3\ell/2$. The RG stops at $r_{\ell_c} \approx 1$ where $e^{\ell_c} \equiv \xi_y$. Integration of (13) between $\ell = 0$ and $\ell = \ell_c$ gives for ξ_y

$$\xi_y = \frac{2}{t\theta^2}\mathcal{T}^{1/3}, \qquad \mathcal{T}(\xi_y) = 1 + \frac{\mathcal{C}_2}{\epsilon K_0}(\xi_y^\epsilon - 1). \qquad (14)$$

For $(\mathcal{C}_2/\epsilon K_0)\xi_y^\epsilon \gg 1$, i.e., inside the critical region of the chiral transition, one finds $\xi_y \sim \theta^{-2}|t_c/t|^{\nu_y}$. To order ϵ,

$$\nu_y^{-1} = (2\nu_x)^{-1} = \gamma^{-1} = 1 - \epsilon/3. \qquad (15)$$

ν_α denotes the correlation length exponent in the α direction. With $K_0 \approx K_c$ we obtain in two dimensions $\mathcal{C}_2/(\epsilon K_c) \approx 0.13\theta^2$ and hence $t_c \approx 0.034\theta^2$ for the size of the critical region. The specific heat exponent $\alpha = \nu_y \epsilon/3$ obeys the hyperscaling relation [20]

$$\nu_x + (d-1)\nu_y = 2 - \alpha, \qquad (16)$$

which applies to the anisotropic system considered here. We have also calculated the exponents $\eta_{x,y}$ defined by the critical propagator $\mathcal{G}^{-1}(\mathbf{k}) = (k_x^{4-\eta_x}/4) + k_y^{2-\eta_y}$ and found to order ϵ^2 $\eta_x = -0.212\epsilon^2$ and $\eta_y = 0$. As expected, all exponents are different from the Onsager values $\alpha = 0$, $\nu = 1$, $\eta = 1/4$.

On larger scales $\ell > \ell_c$, the nonlinear term in (9) is irrelevant. Since $r(\ell_c) = 1$, the effective model on this scale is the standard XY model. The RG flow equations in two dimensions are those of BKT [1],

$$dK_0^{-1}/d\ell = 4\pi^3 z^2, \qquad d\ln z/d\ell = 2 - \pi K_0, \quad (17)$$

where we use isotropic rescaling. These equations have to be integrated with the initial conditions on the scale e^{ℓ_c}. Thus $K_{\ell_c} = K \exp(-\epsilon\ell_c)$ and $z_{\ell_c} \approx \exp(3\ell_c/2 - \bar{E}_{\mathrm{core}})$. Integration of the flow equations gives the following relation for the BKT transition temperature

$$2/(\pi K_{\ell_c}) = 1 + \ln 2 + 2\pi^2 z_{\ell_c}^2 - \ln(\pi K_{\ell_c}). \quad (18)$$

The gapped chiral phase.—Below $T_c = J/K_c$ we rewrite $\phi_x = \kappa + \varphi_x$, where $\kappa = \langle\phi_x\rangle \ll 1$. The expansion of the free energy density with respect to κ can be written as

$$\bar{\mathcal{F}} = \frac{1}{2}K_0 \left[r_0 \mathcal{T}^{-1/3}\kappa^2 + \frac{1}{4}\mathcal{T}^{-1}\kappa^4 \right]. \quad (19)$$

Minimization of $\mathcal{F}$ gives $\kappa^2 = -2r_0\mathcal{T}^{2/3}$. The correlation length is therefore given again by (14) provided t is replaced by $2|t|$. This gives

$$\kappa \equiv \langle\phi_x\rangle \sim |t|^\beta, \qquad \beta = (1-\epsilon)\nu_x. \quad (20)$$

Our exponents fulfill the scaling relation $\alpha + 2\beta + \gamma = 2$.

As already mentioned, previous numerical analysis has ignored the strong anisotropy of the system [17,18] which changes the finite size scaling analysis [21]. By the procedure used in [18] most probably the larger of the two correlation length exponents is obtained, i.e., $\nu_y = 2\nu_x \approx 1$. Then, according to (16), $\alpha \approx 1/2$, whereas using the standard scaling relation with no anisotropy, $\alpha \approx 0.115$ was found in [18]. However, a direct examination of the temperature plots for the specific heat and the order parameter (Figs. 7 and 19 of [18]) gives $\alpha \approx 0.32$, $\beta \approx 0.30$, suggesting $\gamma \approx 1.08$, in reasonable agreement with our values $\alpha = 1/6$, $\beta = 1/3$, $\gamma = 7/6$ when expanded to first order in $\epsilon = 1/2$.

Phase diagram.—At low temperatures we have long range chiral order and a power law decay of spin correlations. This is the chiral nematic (gapless) phase considered in [12,14]. Increasing K_0^{-1} the numerical solution of (18) shows that there is a BKT transition below the chiral transition (see Fig. 1), in qualitative agreement with numerical results [18]. It is important to note that for finding the correct phase boundary the contribution of small scale free vortices ($\ell < \ell_c$) is essential. For $\theta \ll 1$, K_c^{-1}, $K_{\mathrm{KT}}^{-1} \sim \theta^2$, in agreement with [13] (but the opposite sequence of transitions was found there).

Above the BKT transition the spin correlations are short range, the correlation length $\xi_{\mathrm{KT}} \approx e^{1.5/\sqrt{t_{\mathrm{KT}}}}$ is of the order of the vortex distance. Here $t_{\mathrm{KT}} = K_{\mathrm{KT}}/K_0 - 1$. The chiral order parameter vanishes at $T_c = JK_c^{-1}$ that is slightly larger than $T_{\mathrm{KT}} = JK_{\mathrm{KT}}^{-1}$.

In the region $0.25 < K_2/K_0 < 0.316$ there is a reentrant phase transition to the quasiferromagnetic phase (see Fig. 1). It should, however, be taken into account that our approach is restricted to small θ. Thus the size of the

reentrant region may be overestimated when going to larger θ values. Reentrant behavior was seen before using SCHA [13]. However, the SCHA cannot consider vortices accurately and ignores completely the vortex structure on scales smaller ξ.

Antiferromagnetic quantum spin chains.—Using the standard mapping, antiferromagnetic ($J_0 < 0$) spin-S chains at *zero* temperature are described by 1+1 classical systems (4) with the replacements

$$K_0 = \sqrt{2/3}S, \qquad y = v_s\tau, \qquad v_s = \omega_S a, \quad (21)$$

provided $S \gg 1$ [9]. τ denotes the imaginary time, $a = 1$ the lattice constant, v_s the spin-wave velocity, and $\omega_S = \sqrt{3/2}|\theta J_0|S/\hbar$. For increasing K_0 the spin chain undergoes two quantum phase transitions: at K_c from a paramagnetic to helical spin liquid and at K_{KT} to a quasi-long-range ordered magnetic phase (see Fig. 1). The dynamical critical exponents at the quantum phase transitions follows from the relation $\xi_y \sim \xi_x^z$ as $z = 2 - \eta_x/2$ at the chiral, and $z = 1$ at the BKT transition, respectively [24].

Adding a weak interchain coupling $J_\perp = \varepsilon_\perp|J|, \varepsilon_\perp \ll 1$, the system is equivalent to a higher-dimensional classical system. The latter presumably undergoes a single phase transition [10] to a long range ordered magnetic phase. The transition happens at $t = t_{3D}$ which follows from the condition [25] $1 \approx 2J_\perp\chi_{\mathrm{magn}}$, where χ_{magn} denotes the magnetic susceptibility of the 1D chain. This gives $t_{3D} \sim 1/\ln^2\varepsilon_\perp$, in agreement with a more elaborate RG calculation [26].

At low but *finite* T, the imaginary time τ is restricted to the region $0 < \tau < \hbar/T$, i.e., $y < L_y = \hbar\omega_S/T$. At $\varepsilon_\perp = 0$ the system is now equivalent to a one-dimensional classical model and hence no true phases transition can occur. Finite size scaling gives for the susceptibility [24]

$$\chi(K_S, L_y) = \frac{S^2}{|J_0|}\left(\frac{\hbar\omega_S}{T}\right)^{2-\eta_y}\tilde{\chi}\left(\frac{\hbar\omega_S}{T\xi_y}\right). \quad (22)$$

In the quantum critical domain, where $\hbar\omega_S \lesssim T\xi_y$ and $\tilde{\chi}(x) \approx \tilde{\chi}(0)$, $\chi \sim T^{-2+\eta_y}$.

At the chiral transition, with $\chi_{\mathrm{chiral}} \sim \int_{\mathbf{x}} \langle\psi(\mathbf{x})\psi(0)\rangle$, one finds from $\xi_y \approx |t|^{-\nu_y}$ and $\eta_y = 0$ that χ_{chiral} grows as $\sim T^{-2}$ before reaching a maximum at $T \approx T_{p,c} \sim \hbar\omega_S|t|^{\nu_y}$. At the BKT transition where $2 - \eta_y = 7/4$ one obtains analogously $\chi_{\mathrm{magn}} \sim T^{-7/4}$ at $T \gtrsim T_{p,\mathrm{KT}} \sim \hbar\omega_S\exp(-1.5/\sqrt{t_{\mathrm{KT}}})$.

For nonzero interchain coupling, the transition temperature for the magnetic transition is found from $1 = 2J_\perp\chi_{1D}$ and (22) as

$$T_{3D} \approx \hbar\omega_S[\varepsilon_\perp S^2\tilde{\chi}(e^{-1.5/\sqrt{t_{\mathrm{KT}}}}\hbar\omega_S/T_{3D})]^{1/(2-\eta)}. \quad (23)$$

At the BKT transition of the chains, where $t_{KT} = 0$, $T_{3D} \sim \hbar\omega_S\varepsilon_\perp^{4/7}$ which is smaller than the peak temperature T_p by a factor $\varepsilon_\perp^{4/7} \ll 1$. Our result for the $\hbar\omega_S$ and $\varepsilon_\perp$

dependence of T_{3D} agrees with that found in [27] if the mean field exponent $2 - \eta_y = 2$ is used. Other details differ since in [27] spin wave theory was used within the chains.

Experiments.—There is a large number of rare earth metals, alloys, and compounds which exhibit helical phases [28–30]. Unfortunately, experiments on films to our knowledge were done only for cases where the helical axis is perpendicular to the film plane [31]. The other group of materials to which our theory applies are frustrated quantum spin with large S. In $Gd(hfac)_3NITiPr$ half of the spins are $S = 7/2$ and hence sufficiently large, as required, the other half are $S = 1/2$ such that $S_{\text{eff}} \approx \sqrt{7}/2$. Two peaks at $T_N = 1.88$ K and $T_c = 2.19$ K were indeed found in the specific heat of this material [32], which were interpreted as the magnetic and chiral transition, respectively. In contrast our theory explains these peaks as quantum critical phenomena. With $J_0 \approx 7.06$ K, $\varepsilon_\perp \approx 2.3 \times 10^{-3}$, and $\theta \approx 0.36\pi$ [32] one finds $\hbar\omega_S \approx 12.87$ K, $K_0 = 1.08$, $K_c = 1.74$, and $K_{\text{KT}} \approx 2.44$; i.e., at zero temperature the single chains are in their paramagnetic phase (see Fig. 1). $T_{3D} \approx 0.55$ K is much smaller than the observed peak temperatures. The latter are given only up to prefactors of order unity as $T_{p,c} \approx 7.23$ K and $T_{p,\text{KT}} \approx 3.39$ K. The values of the prefactors follow from a calculation of $\tilde{\chi}(x)$, which is beyond the scope of this article.

The other chain compounds have spin $S = 1/2$, resulting in a competition of dimerization and frustration. In some of them the effect of the frustration is dominating. An example is $LiCu_2O_2$ where two nearby transitions have been found as well [33].

In multiferroics the electric polarization **P** is coupled to the magnetisation according to $\mathbf{P} \sim (\mathbf{m} \cdot \nabla)\mathbf{m} - \mathbf{m}(\nabla \cdot \mathbf{m}) \sim \gamma\hat{x}$ [6]. Long range chiral order should be therefore detectable by measuring **P**.

[1] P. Chaikin and T. Lubensky, *Principles of Condensed Matter Physics* (Cambridge, Cambridge, UK, 1995).
[2] J. Villain, J. Phys. II (France) **38**, 385 (1977).
[3] M. Hasenbusch, A. Pelissetto, and E. Vicari1, J. Stat. Mech. (2005) P12002.
[4] S. E. Korshunov, Phys. Usp. **49**, 225 (2006).
[5] L. Balents, Nature (London) **464**, 199 (2010).
[6] M. Mostovoy, Phys. Rev. Lett. **96**, 067601 (2006).
[7] S. Cheong and M. Mostovoy, Nat. Mater. **6**, 13 (2007).
[8] J. Villain, Ann. Isr. Phys. Soc. **2**, 565 (1978).
[9] A. K. Kolezhuk, Prog. Theor. Phys. Suppl. **145**, 29 (2002).
[10] H. Kawamura, J. Phys. Condens. Matter **10**, 4707 (1998).
[11] T. Garel and S. Doniach, J. Phys. C **13**, L887 (1980).
[12] A. K. Kolezhuk, Phys. Rev. B **62**, R6057 (2000).
[13] Y. Okwamoto, J. Phys. Soc. Jpn. **53**, 2613 (1984).
[14] A. A. Nersesyan, A. O. Gogolin, and F. H. L. Eßler, Phys. Rev. Lett. **81**, 910 (1998).
[15] P. Lecheminant, T. Jolicoeur, and P. Azaria, Phys. Rev. B **63**, 174426 (2001).
[16] T. Hikihara, M. Kaburagi, H. Kawamura, and T. Tonegawa, J. Phys. Soc. Jpn. **69**, 259 (2000).
[17] F. Cinti, A. Cuccoli, and A. Rettori, Phys. Rev. B **83**, 174414 (2011).
[18] A. O. Sorokin and A. V. Syromyatnikov, Phys. Rev. B **85**, 174404 (2012); **86**, 059904(E) (2012).
[19] A. M. Ferrenberg and D. P. Landau, Phys. Rev. B **44**, 5081 (1991).
[20] R. M. Hornreich, M. Luban, and S. Shtrikman, Phys. Rev. Lett. **35**, 1678 (1975).
[21] K. Binder and J.-S. Wang, J. Stat. Phys. **55**, 87 (1989).
[22] F. Li, T. Nattermann, and V. L. Pokrovsky, Phys. Rev. Lett. **108**, 107203 (2012).
[23] J. Villain, J. Phys. Chem. Solids **11**, 303 (1959).
[24] S. L. Sondhi, S. M. Girvin, J. P. Carini, and D. Shahar, Rev. Mod. Phys. **69**, 315 (1997).
[25] D. J. Scalapino, Y. Imry, and P. Pincus, Phys. Rev. B **11**, 2042 (1975).
[26] M. Affronte, A. Caneschi, C. Cucci, D. Gatteschi, J. C. Las-jaunias, C. Paulsen, M. G. Pini, A. Rettori, and R. Sessoli, Phys. Rev. B **59**, 6282 (1999).
[27] S. Hikami and T. Tsuneto, Prog. Theor. Phys. **63**, 387 (1980).
[28] J. Jensen and A. Mackintosh, *Rare Earth Magnetism Structures and Excitations* (Oxford University Press, Oxford, UK, 1991).
[29] T. Kimura and Y. Tokura, J. Phys. Condens. Matter **20**, 434204 (2008).
[30] L. C. Chapon, G. R. Blake, M. J. Gutmann, S. Park, N. Hur, P. G. Radaelli, and S.-W. Cheong, Phys. Rev. Lett. **93**, 177402 (2004).
[31] E. Weschke *et al.*, Phys. Rev. Lett. **93**, 157204 (2004).
[32] F. Cinti *et al.*, Phys. Rev. Lett. **100**, 057203 (2008).
[33] T. Masuda, A. Zheludev, A. Bush, M. Markina, and A. Vasiliev, Phys. Rev. Lett. **92**, 177201 (2004).